Conformational Changes in Subdomain 2 of G-Actin: Fluorescence Probing by Dansyl Ethylenediamine Attached to Gln-41

Eldar Kim,* Masao Motoki,‡ Katsuya Seguro,‡ Andras Muhlrad,* and Emil Reisler*
*Department of Chemistry and Biochemistry and the Molecular Biology Institute, UCLA, Los Angeles, CA 90095 USA, and ‡Food Research and Development Laboratories, Ajinomoto Co., Suzuki-cho, Kawasaki-ku, Kawasaki, Kanagawa 210, Japan

ABSTRACT Gln-41 on G-actin was specifically labeled with a fluorescent probe, dansyl ethylenediamine (DED), via transglutaminase reaction to explore the conformational changes in subdomain 2 of actin. Replacement of Ca^{2+} with Mg^{2+} and ATP with ADP on G-actin produced large changes in the emission properties of DED. These substitutions resulted in blue shifts in the wavelength of maximum emission and increases in DED fluorescence. Excitation of labeled actin at 295 nm revealed energy transfer from tryptophans to DED. Structure considerations and Cu^{2+} quenching experiments suggested that Trp-79 and/or Trp-86 serves as energy donors to DED. Energy transfer from these residues to DED on Gln-41 increased with the replacement of Ca^{2+} with Mg^{2+} and ATP with ADP. Polymerization of Mg-G-actin with $MgCl_2$ resulted in much smaller changes in DED fluorescence than divalent cation substitution. This suggests that the conformation of loop 38–52 on actin is primed for the polymerization reaction by the substitution of Ca^{2+} with Mg^{2+} on G-actin.

INTRODUCTION

The atomic structure of G-actin was first solved for an actin:DNaseI complex (Kabsch et al., 1990). The subsequent structures of gelsolin segment 1:actin (McLaughlin et al., 1993) and profilin-β-actin (Schutt et al., 1993) confirmed with only minor modifications the original G-actin structure. Not surprisingly, the main difference in the structure of G-actin in these complexes was traced to the DNaseI binding loop 38–52 and segment 200–207. In the gelsolin segment 1:actin complex these two regions were poorly defined, with residues 40–49 showing no electron density (McLaughlin et al., 1993). This suggests that the 38–52 loop in subdomain 2 of G-actin is mobile or disorded.

The structure and structural transition in this region of subdomain 2 appear important for at least three reasons. First, the original (Holmes et al., 1990) and refined (Lorenz et al., 1993) models of F-actin structure and the ribbon β-actin structure (Schutt et al., 1993) assign an important role to the intermolecular contacts generated between the residues of loop 38–52 and the adjacent monomer. Such contacts and the involvement of this loop in actin polymerization are consistent with the inhibition of polymerization by the modification of His-40 (Hegyi et al., 1974), subtilisin cleavage between residues 47 and 48 (Schwyter et al., 1989), and *Escherichia coli* A2 strain protease cleavage between Gly-42 and Val-43 (Khaitlina et al., 1993). Second, electron microscopy work of Orlova and Egelman (1992, 1993, 1995) and Orlova et al. (1995) implicated the changes in subdomain 2 orientation in the metal- and nucleotide-dependent changes in the flexibility and stability of F-actin. Proteolytic digestion experiments confirmed that the conformation of subdomain 2, and in particular that of loop 38–52 and the sequence 61–69, changes with the substitution of Ca^{2+} with Mg^{2+} and ATP with ADP, in both G-actin (Strzelecka-Golaszewska et al., 1993) and F-actin (Muhlrad et al., 1994). These changes may underlie the known effects of divalent cations and nucleotides on actin polymerization (Estes et al., 1992). Third, the structural model of actin-myosin complex predicts that one of the contacts between these proteins involves residues between His-40 and Gly-42 on actin and Asn-552 and His-558 on myosin (Rayment et al., 1993). In view of the strong evidence for dynamic properties of the 38–52 loop in G- and F-actin and its likely interaction with an adjacent actin monomer in F-actin, the postulated binding of myosin to residues 40–42 on actin could modulate the dynamic behavior of actin filaments (Orlova and Egelman, 1993) and may have important functional implications.

In this work we have taken advantage of the previous finding of Takashi (1988) on specific labeling of Gln-41 on actin via transglutaminase reaction to attach a spectroscopic probe, dansyl ethylenediamine (DED), to this residue. The probe reports on conformational changes in the N-terminal part of the 38–53 loop and broadens significantly the scope of questions about subdomain 2 that can be addressed experimentally. Here, we show large spectral differences between CaATP-, MgATP-, and MgADP-G-actins, and document metal ion- and nucleotide-dependent changes in energy transfer between tryptophan residues and the DED probe on Gln-41 in G-actin. In a separate study we employ

Received for publication 9 May 1995 and in final form 25 July 1995.

Address reprint requests to Dr. Emil Reiser, Department of Chemistry and Biochemistry, University of California, 405 Hilgard Avenue, Los Angeles, CA 90095-1569. Tel.: 310-825-2668; Fax: 310-206-7286; E-mail: reisler@uclach.chem.ucla.edu.

The permanent address of Dr. Muhlrad is Department of Oral Biology, Hadassah School of Dental Medicine, Hebrew University, Jerusalem, 91010, Israel.

Abbreviations used: DED, dansyl ethylenediamine, DNaseI, deoxyribonuclease I, F-actin, filamentous (polymerized) actin; G-actin, monomeric actin; IAEDANS, *N*-(iodoacetyl)-*N'*-(5-sulfo-l-naphthyl)ethylenediamine.

0006-3495/95/11/2024/00 $2.00

the Gln-41 probe for testing the putative interaction of myosin with residues 40–42 on actin.

MATERIALS AND METHODS

Reagents

ATP and ADP, trypsin, and subtilisin Carlsberg were purchased from Sigma Chemical Co. (St. Louis, MO). Bradford reagent was obtained from Bio-Rad (Richmond, CA). 1,5-IAEDANS [*N*-(iodoacetyl)-*N'*-(5-sulfo-l-naphthyl)ethylenediamine] and DED (dansyl ethylenediamine) were from Molecular Probes (Eugene, OR).

Preparation of proteins

Actin from rabbit back muscle was prepared as CaATP-G-actin in Ca-G-buffer (0.5 mM β-mercaptoethanol, 0.2 mM ATP, 0.2 mM $CaCl_2$, and 5 mM Tris-HCl, pH 7.7) according to the method of Spudich and Watt (1971). Microbial transglutaminase was obtained and purified as previously described (Huang et al., 1992). In contrast to transglutaminase from guinea pigs, this enzyme does not require Ca^{2+} for its activity.

DED labeling and the preparation of various forms of actin

CaATP-G-actin (50 μM) was incubated with DED (100 μM) and 0.5 unit/ml of microbial transglutaminase in G-actin buffer supplemented with ATP (up to 0.4 mM). The reaction was carried out for 2 h at room temperature and was stopped by removing the excess of DED on Sephadex G-50 spin columns equilibrated either with Ca-G-buffer (for CaATP-G-actin preparations) or with Mg-G-buffer (0.2 mM EGTA, 0.5 mM β-mercaptoethanol, 0.2 mM ATP, 50 μM $MgCl_2$, and 5 mM Tris-HCl at pH 7.7) (for preparations of MgATP- and MgADP-G-actins). The eluted actin was polymerized by 2.0 mM $CaCl_2$ (for CaATP-G-actin) or 2.0 mM $MgCl_2$ (for MgATP-G-actin) and pelleted in a Beckman airfuge to separate the transglutaminase. The pelleted DED actin was resuspended and depolymerized in either the Ca-G- or Mg-G-actin buffer. The subsequent preparation of CaATP-, MgATP-, and MgADP-(DED)-G-actin followed the procedure of Drewes and Faulstich (1991), as described by Muhlrad et al. (1994). Before use, DED-G-actins were recentrifuged in a Beckman airfuge at 150,000 × *g* for 30 min.

The labeling stoichiometry of G-actin (between 0.90 and 1.05 DED/actin) was determined spectrophotometrically by using the molar extinction coefficient of DED at 334 nm ($\epsilon = 4.8 \times 10^3\ M^{-1}$). The concentration of DED-G-actin was determined by Bradford assay.

Proteolytic digestions of G-actin

Ca- and Mg-G-actins (0.1 mg/ml) were digested with subtilisin at a 500:1 ratio (w/w) of actin to protease, at 25°C in their corresponding Ca-G- and Mg-G buffers. Other conditions, when used, are indicated in the figures. The digestion was stopped at different times with 1 mM phenylmethylsulfonyl fluoride, and the reaction aliquots were analyzed by SDS-PAGE on 10% or 12.5% slab gels. Rates of digestion were determined by densitometric analysis of the undigested actin bands on these gels (Muhlrad et al., 1994) and a single exponential fit of the resulting decay curves for the uncleaved actin. Control subtilisin digestions of a synthetic substrate (*p*-tosyl-L-arginine methylester) in Ca-G- and Mg-G-buffers were used for the correction of G-actin digestion data for small effects of Ca^{2+} and Mg^{2+} on protease activity. Digestions of G-actin (1.0 mg/ml) with trypsin (0.04 mg/ml) were carried out in a Ca-G-actin buffer. These digestions were stopped with soybean trypsin inhibitor and analyzed in the same way as subtilisin digestions of actin.

Fluorescence measurements

All fluorescence measurements were carried out in a Spex Fluorolog spectrofluorometer (Spex Industries, Edison, NJ) at 25°C. Spectra recorded at different protein concentrations should not be numerically compared because of different slit settings.

Analytical ultracentrifugation

Sedimentation velocity experiments were carried out at 56,000 rpm and 25°C in a Beckman Model E analytical ultracentrifuge equipped with a photoelectric scanning system. Sedimentation boundaries of actin (2.0 μM) were recorded at 232 nm. On-line data collection and data analysis was done with a VAX 11/780 computer.

RESULTS

Characterization of DED-labeled actin

Earlier modification of Gln-41 on actin with dansyl cadaverine was carried out with the Ca^{2+}-dependent guinea pig transglutaminase (Takashi, 1988). Because a shorter probe (DED) and a Ca^{2+}-independent bacterial transglutaminase were employed in this work, the labeling of Gln-41 on actin was reexamined. Fig. 1 shows the incorporation of DED into Ca-G-actin and Ca-F-actin. In analogy to the previous study (Takashi, 1988), the labeling of Ca-G-actin by DED is rapid and saturates at 1.00 ± 0.05 DED:actin. In contrast to this and the earlier work, the labeling of F-actin by DED was much slower, and even after a 160-min reaction only a small fraction of actin was modified. It appears that the earlier, much more efficient labeling of Gln-41 on F-actin by dansyl cadaverine (Takashi, 1988) might have been

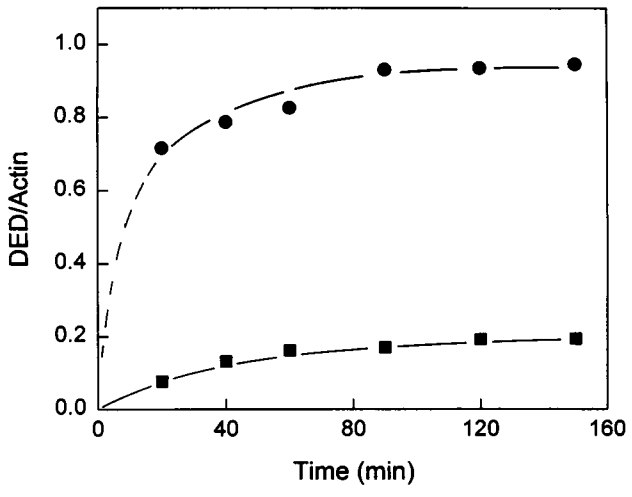

FIGURE 1 DED labeling of G- and F-actin via transglutaminase reaction. The labeling of Ca-G- and Mg-F-actin (2.0 mg/ml) with DED (100 μM) was carried out in the presence of 0.5 unit/ml of microbial transglutaminase at 23°C. Ca-G-actin (●) was labeled in Ca-G-actin buffer containing 0.4 mM ATP; F-actin (■) was modified in the same buffer supplemented with 2.0 mM $MgCl_2$. Labeling stoichiometry (molar ratios of DED/actin) was determined spectrophotometrically on aliquots of the reaction mixture after TCA (10%) precipitation of actin and its resuspension in 0.05 M NaOH.

caused by incomplete polymerization of Ca-G-actin by Ca^{2+} under the conditions employed in that work.

The results of DED modifications shown in Fig. 1 suggested that Gln-41 labeling should be carried out on G-actin. The specificity of such labeling for Gln-41 (Takashi, 1988) was checked by subtilisin cleavage of DED-labeled G-actin between Met-47 and Gly-48. The smaller, 47-residue fragment contains a single glutamine residue at position 41. If the labeling is indeed specific for Gln-41, then the larger, 35-kDa fragment of actin should not carry any fluorescent probe. The inset to Fig. 2 shows that the labeling specificity in our system is as good as previously described (Takashi, 1988). The fluorescence image (lane 5) of the cleaved DED-G-actin products obtained after a 15-min subtilisin digestion reaction does not reveal any probe in the 35-kDa actin fragment (residues 48–374). The fluorescent label can only be detected in either the smaller N-terminal 9-kDa actin fragment (residues 1–47) or in the intact actin. This result and the equimolar labeling of G-actin by DED confirm the specificity of Gln-41 modification in the transglutaminase reaction.

Kinetic analysis of subtilisin cleavage of Ca-G-actin and the DED-labeled G-actin is shown in Fig. 2. The progress of actin digestion was monitored by densitometric scanning of SDS gels of the reaction aliquots. Representative gels of such a digestion reaction, after a 5-min subtilisin cleavage of actin, are shown in lanes 2 and 3 of the inset to Fig. 2. Clearly, identical cleavage products were generated in digestions of both labeled and unlabeled actin. The plots of undigested actin vs. time fitted a single exponential expression and yielded the first-order cleavage rates of 0.30 ± 0.03 min^{-1} and 0.12 ± 0.01 min^{-1} for the unmodified and DED-labeled G-actin. Thus, the labeling of Gln-41 by DED decreased by about 2.5-fold the rate of subtilisin cleavage of G-actin between Met-47 and Gly-48.

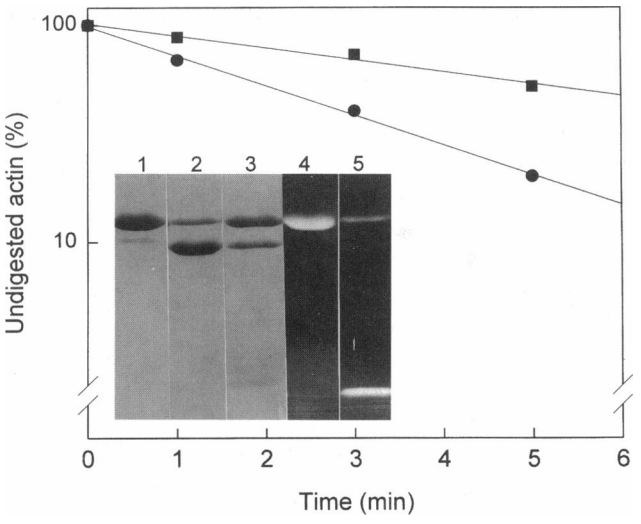

FIGURE 2 Time dependence of subtilisin digestion of G-actin. Unlabeled (●) and DED-labeled (■) Ca-ATP-G-actins (1.0 mg/ml) were digested with subtilisin (1.0 μg/ml) in Ca-G-actin buffer at 23°C. The amount of uncleaved actin in each reaction aliquot was determined by densitometric analysis of actin bands on SDS PAGE. The cleavage rates for unlabeled and DED-labeled actin were 0.30 ± 0.03 and 0.12 ± 0.01 min^{-1}, respectively. Inset: representative gels of the digestion reaction. Lanes 1–3 show Coomassie blue-stained undigested actin (1), unlabeled actin after 5 min of cleavage (2), and DED-labeled actin cleaved for 5 min (3). Only the intact actin (*upper band*) and the main 35-kDa cleavage product are visualized on these gels. Lanes 4 and 5 show the fluorescence images of undigested and digested (15 min) DED-labeled G-actin.

Previous proteolytic digestion studies on G-actin demonstrated a structural relationship between loop 38–52 and the tryptically sensitive region between Lys-61 and Lys-68 on actin (Strzelecka-Golaszewska et al., 1993). To test the extent of structural perturbation of subdomain 2 by Gln-41 labeling, tryptic digestions of unmodified and DED-labeled G-actin were compared. The same products and similar digestion rates (not shown) were observed for both materials. This shows that Gln-41 labeling introduces only local changes in the loop 38–52 and that these changes do not spread to the Lys-61 and Lys-68 region.

Metal- and nucleotide-dependent conformational changes in subdomain 2 of G-actin

Emission spectra of DED-labeled actin in the CaATP, MgATP, and MgADP forms of G-actin are shown in Fig. 3. All spectra were recorded at 1.0 μM protein concentrations and with λ_{ex} = 334 nm. The spectra reveal striking differences in the environment of the Gln-41 probe in the three forms of G-actin. These changes are considerably larger than the previously observed spectral perturbations of Cys-374 probes caused by similar replacements of Ca^{2+} with Mg^{2+} and ATP with ADP on G-actin (Carlier et al., 1986; Zimmerle et al., 1987; Estes et al., 1987). The increases in the quantum yield of DED and the blue shifts in the λ_{max}

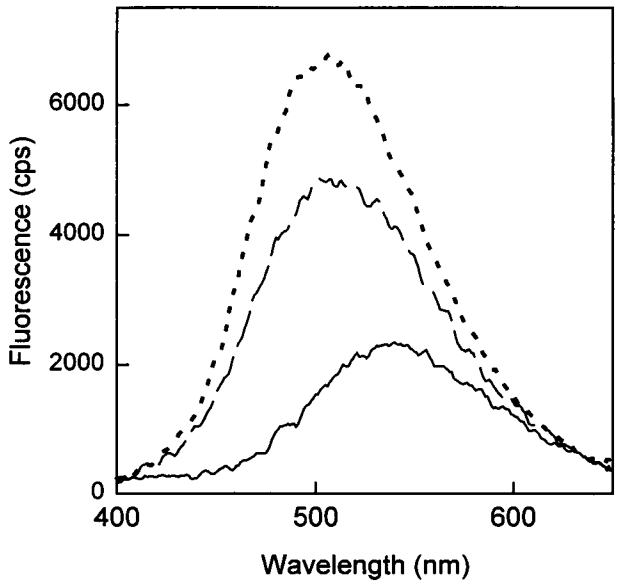

FIGURE 3 Emission spectra of DED-labeled G-actin. Solid trace, CaATP-G-actin; dashed trace, MgATP-G-actin; dotted trace, MgADP-G-actin. All spectra were taken at 1.0 μM G-actin with λ_{ex} = 334 nm.

values of its emission, upon replacement of Ca^{2+} (λ_{max} = 536 nm) by Mg^{2+} (λ_{max} = 511 nm) in ATP-G-actin, or ATP with ADP (λ_{max} = 507 nm) in Mg-G-actin, suggest a transfer of the probe to a more hydrophobic environment and a partial rearrangement of the 38–52 loop. This rearrangement is also indicated by fluorescence polarization measurements (λ_{ex} = 334, λ_{em} = 520 nm), which yielded anisotropy values of 0.178, 0.200, and 0.205 for CaATP-, MgATP-, and MgADP-G-actins.

Previous proteolytic digestion experiments showed metal- and nucleotide-dependent changes at the subtilisin cleavage site, between Met-47 and Gly-48, and in the 61–68 region on actin (Strzelecka-Golaszewska et al., 1993). Thus, the spectral changes shown in Fig. 3 can be related to larger, overall transitions in loop 38–52. This was confirmed by observing a threefold slower subtilisin cleavage of MgATP-labeled than that of CaATP-labeled and unlabeled G-actin (not shown).

Because the polymerization of DED-G-actin is also accompanied by an increase in the quantum yield of the probe, it is important to establish that the metal and nucleotide substitutions in G-actin do not cause its oligomerization. To avoid such a risk, the emission spectra were taken in most cases at 1.0 μM actin, i.e., below its critical concentration for polymerization at the Ca^{2+} and Mg^{2+} concentrations used in this work (Attri et al., 1991). Importantly, also, sedimentation velocity experiments did not detect the presence of oligomers in G-actin solutions. Sedimentation boundaries recorded at λ = 232 nm and at an actin concentration of 2.0 μM (at 25°C) did not reveal any fast sedimenting component in unlabeled CaATP-G-actin and DED-labeled CaATP-, MgATP-, and MgADP-G-actin. All actins sedimented as monomers, with $s_{20°,w}$ = 3.20 ± 0.10S (Attri et al., 1991). Thus, it may be concluded that the spectra presented in Fig. 3 show conformational changes between monomeric forms of G-actin. Also, the identical $s_{20°,w}$ values suggest that the anisotropy differences between CaATP- and MgATP-DED-G-actins reflect local changes around the probe and its greater immobilization in the MgATP-actin monomer.

Energy transfer from tryptophans to DED on Gln-41

Excitation of MgATP-DED-G-actin at 295 nm produced two emission bands, the tryptophan band centered at 340 nm and the DED peak with λ_{max} at 511 nm (Fig. 4, dashed trace). The intensity of DED fluorescence was higher when excited at 295 nm than at the λ_{max} for the excitation of this probe (334 nm). This suggested energy transfer from actin's tryptophans to the Gln-41 probe. Such an energy transfer was confirmed by recording tryptophan fluorescence of unlabeled MgATP-G-actin (Fig. 4, solid trace) under identical experimental conditions. The decreased intensity of tryptophan emission at 340 nm in DED-G-actin, compared to that of unlabeled actin, can be ascribed to energy transfer to DED.

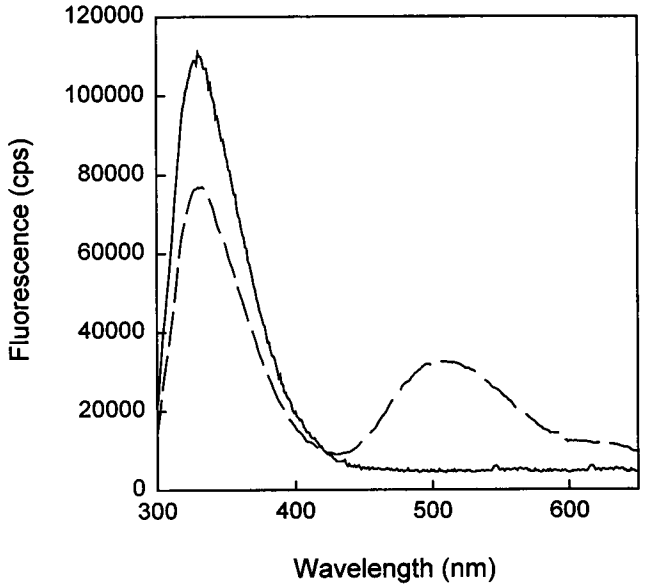

FIGURE 4 Emission spectra of Mg-ATP G-actin excited at 295 nm. Solid trace, unlabeled MgATP-G-actin (5.0 μM); dashed trace, DED-labeled MgATP-G-actin (5.0 μM).

A comparison of emission spectra of 1.0 μM DED-G-actin (λ_{ex} = 295 and 334 nm) for the CaATP, MgATP, and MgADP monomers (Figs. 3 and 5) reveals energy transfer from tryptophans to DED in all cases. It is instructive to compare the ratios of emission intensities at λ_{em} = 530 nm for excitations at 295 and 334 nm. These ratios, $I_{ex,295}/I_{ex,334}$, derived from excitation spectra of free DED (in Mg-G-actin buffer) and 1.0 μM DED-actins (data not shown), and multiplied by a factor of 1.65 to account for the different absorption coefficients of DED at 295 and 334 nm, were 1.09, 1.70, 2.40, and 2.60 for free DED and CaATP-,

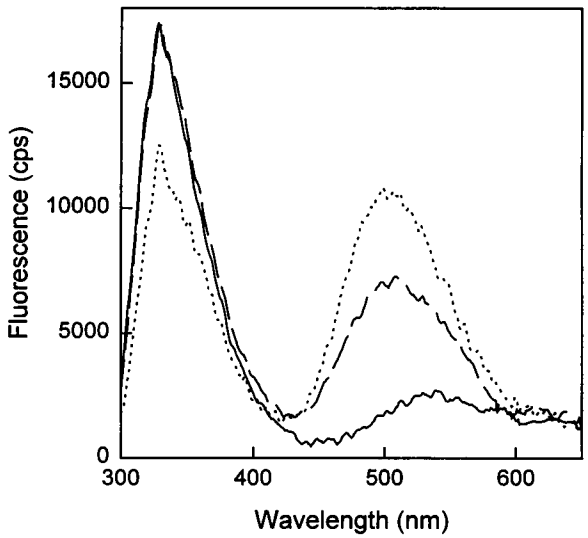

FIGURE 5 Emission spectra of DED-labeled G-actin. All spectra were taken at 1.0 μM G-actin with λ_{ex} = 295 nm. Solid trace, CaATP-G-actin; dashed trace, MgATP-G-actin; dotted trace, MgADP-G-actin.

MgATP-, and MgADP-labeled G-actins, respectively. These ratios verify energy transfer from tryptophans to DED and indicate that the efficiency of this process increases with the replacement of Ca^{2+} by Mg^{2+} and ATP by ADP. A better estimate of energy transfer changes is obtained from the tryptophan fluorescence of G-actin in the presence and absence of DED (Fig. 4 and similar plots for CaATP- and MgADP-G-actin). The efficiencies of energy transfer calculated from such spectra (R_o = 21 Å; Wu and Brand, 1994) are 21.4%, 31.2%, and 40.7% for CaATP-, MgATP-, and MgADP-G-actin, respectively. As documented below, these changes in energy transfer probably reflect the changes in a distance between DED on Gln-41 and Trp-79 and/or Trp-86.

Tryptophans 79, 86, 340, and 356 on G-actin and energy transfer to DED on Gln-41

Distance considerations based on the atomic structure of G-actin (Kabsch et al., 1990) and the Forster distance (R_o = 21A; Wu and Brand, 1994) for the dansyl-tryptophan pair lead to the prediction of theoretical efficiencies of energy transfer from actin's tryptophans to DED on Gln-41 (Table 1). These calculations have only limited value because they are based on the atomic position of Gln41 in the DNaseI:actin complex (Kabsch et al., 1990). The position of Gln-41 is most likely different in the uncomplexed actin (McLaughlin et al., 1993) and is probably changed by DED labeling. Also, the relative contribution of each tryptophan to the overall tryptophan quantum yield of G-actin is not known, further complicating numerical analysis of their respective energy transfer contributions. Despite these qualifications, the theoretical efficiencies of energy transfer suggest that only Trp-79 and/or Trp-86 participates in this process.

This conclusion can be checked by quenching the tryptophan fluorescence in G-actin by Cu^{2+} (Lehrer and Kerwar, 1972). The quenching is due to a strong and specific Cu^{2+} binding to Cys-374 on actin and its spectral overlap with tryptophan emission. The quenching should be efficient for Trp-340 and Trp-356, which are located 18.2 Å and 15.2 Å from Arg-372, respectively, i.e., within Forster distance for the Cu^{2+}-tryptophan pair (20 Å; Lehrer and Kerwar, 1972). (The distance from tryptophans to Arg-372 instead of to Cys-374 is measured because the atomic structure of G-actin lacks the last three residues.) If Trp-340 and Trp-356 transfer energy to DED on Gln-41 then the quenching of their fluorescence by Cu^{2+} should decrease the transfer of energy. Emission spectra of 1:1 complexes of MgATP (DED) G-actin (Fig. 6 *a*) and CaATP-(DED)-G-actin (not shown) with Cu^{2+} do not reveal any significant spectral changes in the DED band using both λ_{ex} = 295 and 334 nm. In the latter case (λ_{ex} = 334) perturbation of DED fluorescence by Cu^{2+} was indeed not expected because of the lack of spectral overlap between them. However,

TABLE 1 Calculated efficiencies of energy transfer from actin's tryptophans to DED on Gln-41

Tryptophan	Distance Å	Efficiency of transfer (%)
Trp-79	24.8	26.9
Trp-86	25.4	24.2
Trp-340	40.0	2.1
Trp-356	44.8	1.0

The distance from Gln-41 to actin's tryptophans was determined by using the KINEMAGE program and the atomic coordinates of G-actin (Kabsch et al., 1990). The Forster distance for the dansyl-tryptophan pair, R_o = 21Å, was taken from Wu and Brand (1994).

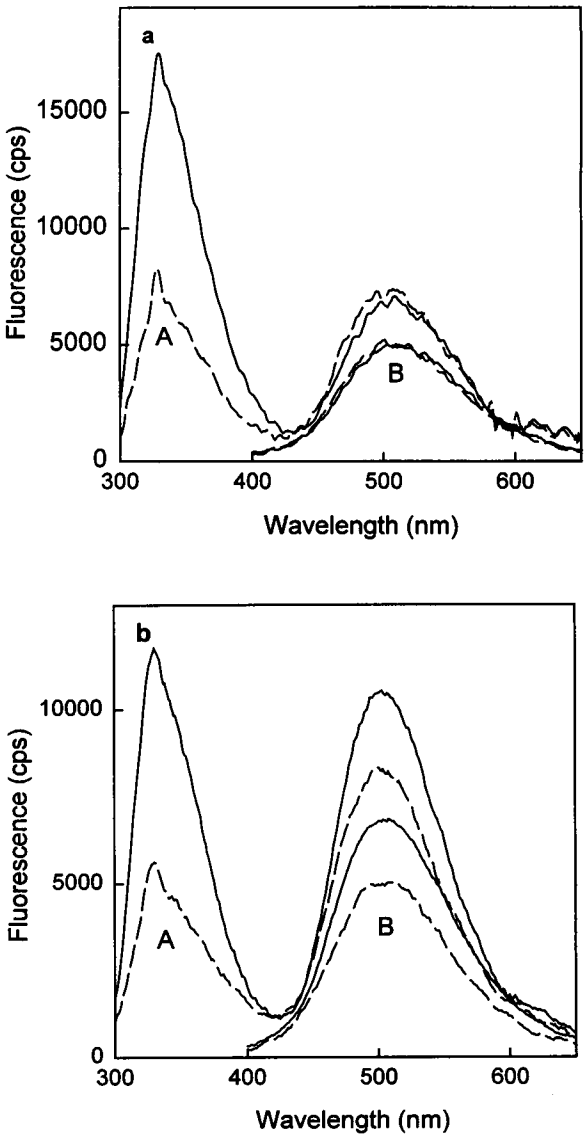

FIGURE 6 Emission spectra of DED-labeled G-actin in the presence and absence of Cu^{2+}. (*a*) Spectra of MgATP-G-actin (1.0 μM) in the absence (*solid trace*) and presence (*dashed trace*) of 1.0 μM Cu^{2+}. The spectra were recorded with λ_{ex} set at 295 nm (*A traces*) and 334 nm (*B traces*). (*b*) Spectra of MgADP-G-actins (1.0 μM) in the absence (*solid trace*) and presence (*dashed trace*) of 1.0 μM Cu^{2+}. The spectra were recorded with λ_{ex} set at 295 nm (*A traces*) and 334 nm (*B traces*).

the strong quenching by Cu^{2+} of tryptophan emission (λ_{em} = 340 nm) in the labeled MgATP-G-actin (Fig. 6 *a*, A traces) without a significant change in the DED fluorescence peak supports the conclusion derived from Table 1 that Trp-340 and Trp-356 are unlikely to transfer energy to DED on Gln-41. Thus, it appears that metal-dependent changes in energy transfer from tryptophans to DED originate from changes in the distance between Trp-79 and/or Trp-86 and DED on Gln-41 in G-actin.

Cu^{2+} probing of MgADP-G-actin

As shown in Figs. 3 and 5, the substitution of ATP by ADP in Mg-DED-G-actin induced changes in DED fluorescence and in the energy transfer from tryptophans to DED (Fig. 5). In contrast to CaATP- and MgATP-G-actins (Fig. 6 *a*), the DED fluorescence of MgADP-G-actin was partially quenched by equimolar amounts of Cu^{2+} for emission spectra taken at both λ_{ex} = 295 nm (Fig. 6 *b*, A traces) and λ_{ex} = 334 nm (Fig. 6 *b*, B traces). In the latter case, the effect of Cu^{2+} must indicate a structural perturbation of the Gln-41 region because there is no spectral overlap between the probe and the metal. This result can be rationalized by the findings of Drewes and Faulstich (1991). These authors reported on local, reversible perturbation, and/or unfolding, in MgADP-G-actin, which leads to a specific exposure of Cys-10 on actin to thiol reagents and a reduced inhibition of DNase I activity.

To verify that the quenching of DED-MgADP-G-actin fluorescence by Cu^{2+} is related to its binding to cysteine residues other than Cys-374, we employed IAEDANS-labeled G-actin. The modification of Cys-374 by IAEDANS blocks the binding of Cu^{2+} to this residue. Accordingly, addition of Cu^{2+} to IAEDANS-labeled CaATP-G-actin did not result in any significant quenching of tryptophan and IAEDANS fluorescence (Fig. 7 *a*). On the other hand, addition of Cu^{2+} to the MgADP form of IAEDANS-labeled actin caused a significant quenching of IAEDANS and some decrease in tryptophan fluorescence (Fig. 7 *b*). This result is consistent with the reported structural differences between MgADP and MgATP-G-actins (Drewes and Faulstich, 1991) and suggests that DED quenching by Cu^{2+} in MgADP-G-actin may be caused by the binding of metal to the exposed Cys-10 residue and the resulting changes in actin and particularly in the environment of Gln-41.

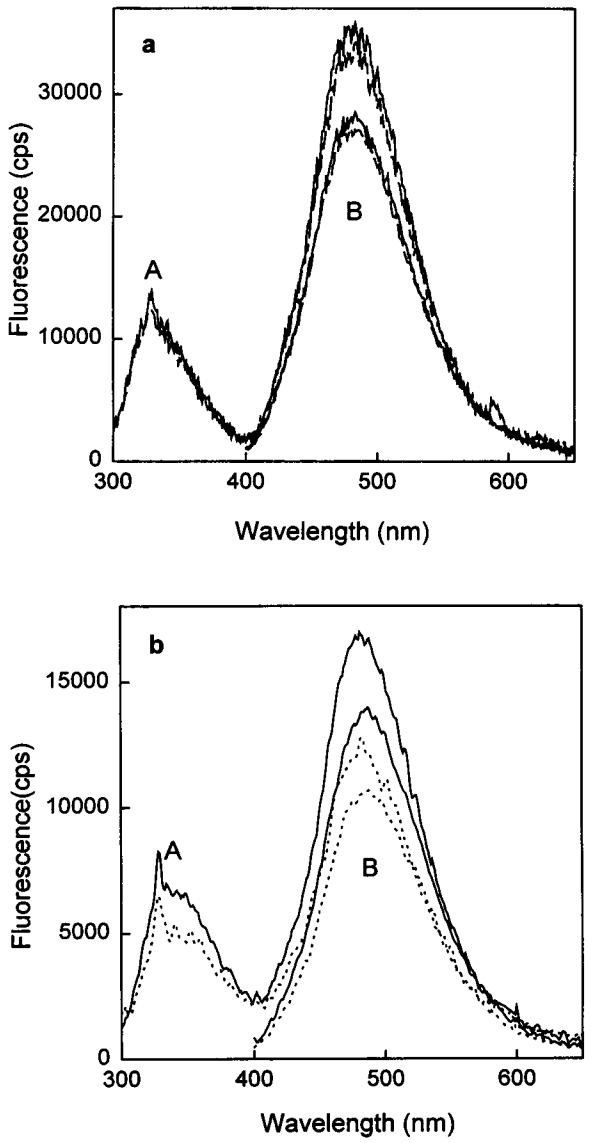

FIGURE 7 Emission spectra of IAEDANS-labeled G-actin in the presence and absence of Cu^{2+}. (*a*) Spectra of MgATP-G-actin (1.0 μM) in the absence (*solid trace*) and presence (*dashed trace*) of 1.0 μM Cu^{2+}. The spectra were recorded with λ_{ex} set at 295 nm (*A traces*) and 337 nm (*B traces*). (*b*) Spectra of MgADP-G-actin (1.0 μM) in the absence (*solid trace*) and presence (*dashed trace*) of 1.0 μM Cu^{2+}. The spectra were recorded with λ_{ex} set at 295 nm (*A traces*) and 337 nm (*B traces*).

Polymerization of G-actin alters the environment of Gln-41

It has been reported before that the polymerization of dansyl-cadaverine-labeled CaATP-G-actin by Mg^{2+} is accompanied by a twofold increase in the fluorescence of the Gln-41 probe and a blue shift in its λ_{max} (Takashi, 1988). As shown in this work, the substitution of Ca^{2+} by Mg^{2+} in G-actin causes similar changes in DED fluorescence. Thus, to detect polymerization-related changes in the Gln-41 environment, MgATP- and CaATP-G-actins were polymerized with 2.0 mM $MgCl_2$ and $CaCl_2$, respectively. Fig. 8 shows DED spectra of MgATP-G-actin and Mg-F-actin (both at 5.0 μM) after excitation at λ_{ex} = 334 nm (B traces) and 295 nm (A traces). The polymerization of G-actin induced a small increase in the fluorescence intensity of DED (for λ_{ex} = 334 nm) and a λ_{max} shift from 511 to 520 nm. The fluorescence increase is significantly larger upon excitation of G- and F-actin at 295 nm because of the readily visible increase in energy transfer from tryptophans to DED (Fig. 8, group A traces). It should be noted, however, that the polymerization of unlabeled Mg-G-actin is

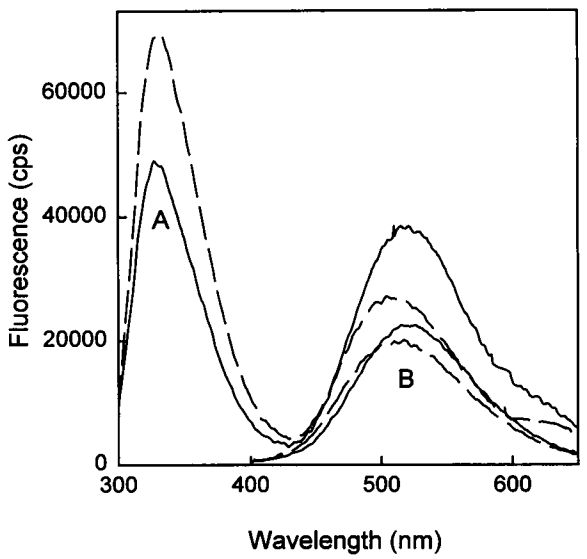

FIGURE 8 Emission spectra of DED-labeled G- and F-actins. The spectra of MgATP-G-actin (*dashed trace*) and Mg-F-actin (*solid trace*) were recorded at 5.0 μM actin with λ_{ex} set at 295 nm (*A traces*) and 334 nm (*B traces*).

accompanied by an approximately 25% decrease in tryptophan emission at 340 nm (see also Lynn et al., 1994). Thus, only about a 15% decline in the intensity of tryptophan fluorescence in Mg-F-actin can be ascribed to the increased energy transfer to DED. The attribution of this increase in energy transfer to changes in distance is complicated by the possible contribution of Trp-340 and/or Trp-356 to that process in F- but not in G-actin. This possibility is supported by a significant decrease in energy transfer to DED by Cu^{2+} in F-actin (data not shown) and not in MgATP-G-actin.

In contrast to relatively small changes in DED fluorescence of MgATP-G-actin with actin polymerization (Fig. 8, group B traces), the fluorescence of this probe was blue shifted and increased by about twofold upon polymerization of CaATP-G-actin by $CaCl_2$ (data not shown). These results suggest that the conformation of the 38–52 loop (or its N-terminal part) in Mg-G-actin may be closer to that in F-actin than in Ca-G-actin.

DISCUSSION

The goal of this work has been to introduce a fluorescent probe into the 38–52 loop on actin and employ it for the exploration of conformational states of subdomain 2. The interest in this region of actin is related to the recent demonstration that subdomain 2, and the loop 38–52 and segment 61–69 in particular, undergo divalent cation-dependent and nucleotide-dependent changes in their proteolytic susceptibilities (Strzelecka-Golaszewska et al., 1993). The changes induced by Mg^{2+} could be interpreted as a "folding inward" of loop 38–52, which is either highly mobile or not structured in CaATP-G-actin (McLaughlin et al., 1993). Importantly, also, the changes in subdomain 2 of G-actin could be linked to the known effects of $MgCl_2$ and ADP on the polymerization of actin and its inhibition by various modifications of subdomain 2 residues (Strzelecka-Golaszewska et al., 1993). Moreover, as elegantly demonstrated by Orlova and Egelman (1993), Mg^{2+}- and Ca^{2+}- polymerized actin filaments show different structural stabilities and orientations of subdomain 2.

MgATP-G-actin

The results of this work provide spectroscopic evidence for conformational changes around Gln-41 on actin upon replacement of Ca^{2+} with Mg^{2+} and ATP with ADP in G-actin. The large changes in fluorescence intensity and λ_{max} of DED emission observed for these conversions called for special attention to the possible oligomerization of actin by Mg^{2+} and ADP. Such a possibility was minimized by working well below the critical concentration for polymerization of G-actin (12.5 μM at 100 μM $MgCl_2$; Attri et al., 1991); most spectra were recorded at 1.0 μM G-actin, in the presence of 50 μM $MgCl_2$, after only a brief equilibration to 25°C. More importantly, sedimentation velocity experiments ruled out the presence of any significant fraction of oligomers in G-actin solutions. Finally, the polymerization of Mg-G-actin by $MgCl_2$ resulted in a small but signficant red shift in λ_{max} of DED, from 511 to 520 nm, i.e., in a direction opposite that of the change associated with CaATP- to MgATP-G-actin conversion (Fig. 8).

The above considerations lead to the conclusion that the major change in the Gln-41 region on actin occurs with the formation of Mg-G-actin, and its subsequent polymerization is accompanied by a smaller perturbation of this site. In other words, according to DED fluorescence, the N-terminal part of loop 38–52 assumes an "F-actin-like" state in Mg-G-actin. Notably, tryptic digestion of Ca-G-actin and Mg-G-actin provided similar information on segment 61–69 on actin, revealing its considerable protection from cleavage in Mg-G-actin (Strzelecka-Golaszewska et al., 1993). Thus, it appears that a significant part of subdomain 2, not just the Gln-41 site, assumes "F-actin-like" conformation in Mg-G-actin, facilitating its polymerization into filaments. Such a possibility was raised in earlier studies (Estes and Gershman, 1978), but in that work actin was probably in the oligomeric form (Newman et al., 1985; Attri et al., 1991).

Additional information on nucleotide- and divalent cation-induced changes in the structure of subdomain 2 on actin can be derived from energy transfer from tryptophans to DED documented in this work. Despite uncertainties related to the atomic coordinates of Gln-41 in G-actin free of DNaseI, and after DED labeling, the predicted efficiencies of energy transfer from actin's tryptophans to DED are instructive (Table 1). These estimates, which show that energy transfer to DED on Gln-41 in G-actin must be limited to Trp-79 and/or Trp-86, are supported by Cu^{2+} quenching experiments (Fig. 6 *a*). The efficiency of energy

transfer in CaATP-G-actin (21.4%) is in good agreement with the efficiency calculated for Trp-79 and/or Trp-86 in Table 1. More importantly, energy transfer measurements suggest that the distance between Gln-41 and Trp-79 and/or Trp-86 decreases in MgATP and MgADP-G-actins relative to that in Ca-ATP-G-actin. Quantitative estimates of such movements are not warranted because of the possible involvement of two tryptophan donors in the energy transfer process and four tryptophans in tryptophan fluorescence. However, these results strengthen the conclusion on a significant structural rearrangement of subdomain 2 in G-actin. It is pertinent to note that Mg-induced changes in G-actin are not limited to subdomain 2; they spread to the 18–29 (Mejean et al., 1988; Adams and Reisler, 1994) and C-terminal (Strzelecka-Golaszewska et al., 1993) segments of subdomain 1.

MgADP-G-actin

The replacement of ADP with ATP in Mg-G-actin resulted in additional changes, an increase in the fluorescence of DED, a blue shift in the λ_{max} of its emission (from 511 to 507 nm), and an increase in energy transfer from tryptophans to DED. In contrast to these incremental spectral changes, Cu^{2+} quenching of tryptophan emission had qualitatively different effects on DED fluorescence in MgADP- and MgATP-G-actins. In MgADP-G-actin, but not in MgATP-G-actin, the quenching of tryptophan fluorescence by Cu^{2+} was accompanied by a partial loss of energy transfer to DED (Fig. 6 *b*). However, because Cu^{2+} quenched DED fluorescence on MgADP-G-actin also more directly, after excitation at $\lambda = 334$ nm, it was clear that additional factors contribute to the spectral changes in MgADP-G-actin. This contention was verified by showing that in G-actin labeled with IAEDANS at Cys-374 Cu^{2+} quenched tryptophan and IAEDANS fluorescence in MgADP-G-actin but not in Ca-ATP- and MgATP-G-actin. On the assumption that Cu^{2+} is chelated to Cys-10 (Drewes and Faulstich, 1991) in MgADP-G-actin, our results suggest that such a chelation causes, or perhaps amplifies widely spread changes in actin, including those occurring at the Cys-374 and Gln-41 sites. Changes in the DNase I binding site on G-actin after the exposure of Cys-10 to thiol reagents in MgADP-G-actin were also reported by Drewes and Faulstich (1991).

Polymerization of G-actin

As indicated before, the polymerization of MgATP-G-actin by $MgCl_2$ shifts the λ_{max} of DED emission and results in a small increase in the fluorescence of this probe. A much larger spectral change, associated with the polymerization of Mg-G-actin, which reflects an increase in energy transfer from tryptophans to DED (Fig. 8), raises a question about possible changes in the distance between the probe and tryptophans. However, the interpretation of such changes is complicated by the fact that according to the model of F-actin structure (Holmes et al., 1990; Lorenz et al., 1993; Tirion et al., 1995), additional tryptophans (Trp-340 and Trp-356) could become energy donors to DED in the actin polymer. This possibility has been verified by the observation that Cu^{2+} bound to Cys-374 reduced energy transfer from tryptophans to DED in Mg-F- but not in Mg-G-actin. Such a quenching in the polymer can be easily rationalized if Trp-340 and/or Trp-356 become energy donors to DED; these residues are readily quenched by Cu^{2+}. These results and considerations do not preclude a change in distance between Gln-41 and Trp-79 and/or Trp-86 upon actin polymerization. It can be predicted on the basis of the Lorenz et al. (1993) model of F-actin structure that the distance between Gln-41 and Trp-86 should remain invariant and that between Gln-41 and Trp-79 should increase by close to 3 Å upon polymerization of actin. Interestingly, as shown in this work, the substitution of Ca^{2+} with Mg^{2+} on G-actin leads to an opposite change, a decrease in the distance between Gln-41 and Trp-79 and/or 86.

In conclusion: our results show that DED labeling of Gln-41 provides a sensitive probe of conformational rearrangements in subdomain 2 of actin. Our results document large spectroscopic changes associated with the replacement of Ca^{2+} with Mg^{2+} and ATP with ADP and show that these substitutions change the position of Gln-41 with respect to Trp-79 and/or Trp-86. Moreover, the spectral data reveal that the major change in the environment of Gln-41 occurs with the conversion of Ca-G-actin to Mg-G-actin, perhaps priming this site for the polymerization of actin. Additional, albeit smaller changes occur in this region with the polymerization of actin.

This work was supported by grant MCB 9206739 from the National Science Foundation.

REFERENCES

Adams, S., and E. Reisler. 1994. Sequence 18–29 on actin: antibody and spectroscopic probing of conformational changes. *Biochemistry.* 33: 14426–14433.

Attri, A. K., M. S. Lewis, and E. D. Korn. 1991. The formation of actin oligomers studied by analytical ultracentrifugation. *J. Biol. Chem.* 266: 6815–6824.

Carlier, M.-F., D. Pantaloni, and E. D. Korn. 1986. Fluorescence measurements of the binding of cations to high-affinity and low-affinity sites on ATP-G-actin. *J. Biol. Chem.* 261:10778–10784.

Drewes, G., and H. Faulstich. 1991. A reversible conformational transition in muscle actin is caused by nucleotide exchange and uncovers cysteine in position 10. *J. Biol. Chem.* 266:5508–5513.

Estes, J. E., and L. C. Gershman. 1978. Activation of heavy meromyosin adenosine triphosphatase by various states of actin. *Biochemistry.* 17: 2495–2499.

Estes, J. E., L. A. Selden, and L. C. Gershman. 1987. Tight binding of divalent cations to monomeric actin. *J. Biol. Chem.* 262:4952–4957.

Estes, J. E., L. A. Selden, H. J. Kinosian, and L. C. Gershman. 1992. Tightly-bound divalent cation of actin. *J. Muscle Res. Cell Motil.* 13: 272–284.

Hegyi, G., G. Premecz, B. Sian, and A. Muhlrad. 1974. Selective carbethoxylation of histidine residues on actin by diethylpyrocarbonate. *Eur. J. Biochem.* 44:7–12.

Holmes, K. C., D. Popp, W. Gebhard, and W. Kabsch. 1990. Atomic model of the actin filament. *Nature.* 347:44–49.

Huang, Y.-P., K. Seguro, M. Motoki, and K. Tawada. 1992. Cross-linking of contractile proteins from skeletal muscle by treatment with microbial transglutaminase. *J. Biochem. (Tokyo).* 112:229–234.

Kabsch, W., H. G. Mannherz, D. Suck, E. F. Pai, and K. C. Holmes. 1990. Atomic structure of the actin: DNase I complex. *Nature.* 347:37–44.

Khaitlina, S. Y., J. Moraczewska, and H. Strzelecka-Golaszewska. 1993. The actin/actin interactions involving the N-terminus of the DNase1 binding loop are crucial for stabilization of the actin filament. *Eur. J. Biochem.* 218:911–920.

Lehrer, S. S., and G. Kerwar. 1972. Intrinsic fluorescence of actin. *Biochemistry.* 11:1211–1217.

Lorenz, M., D. Popp, and K. C. Holmes. 1993. Refinement of the F-actin model against x-ray fiber diffraction data by the use of a directed mutation alogarithm. *J. Mol. Biol.* 234:826–836.

Lynn, A. S., H. J. Kinosian, J. E. Estes, and L. C. Gershman. 1994. Influence of the high affinity divalent cation on actin tryptophan fluorescence. *Adv. Exp. Med. Biol.* 358:51–57.

McLaughlin, P. J., J. I. Gooch, H. G. Mannherz, and A. G. Weeds. 1993. Structure of gelsolin segment 1-actin complex and the mechanism of filament severing. *Nature.* 364:685–692.

Mejean, C., H. K. Hue, F. Pons, C. Roustan, and Y. Benyamin. 1988. Cation binding sites on actin: a structural relationship between antigenic epitopes and cation exchange. *Biochem. Biophys. Res. Commun.* 152: 368–375.

Muhlrad, A., P. Cheung, B. C. Phan, C. Miller, and E. Reisler. 1994. Dynamic properties of actin: structural changes induced by beryllium fluoride. *J. Biol. Chem.* 269:11852–11858.

Newman, J., J. E. Estes, L. A., Selden, and L. C. Gershman. 1985. Presence of oligomers at subcritical actin concentrations. *Biochemistry.* 24: 1538–1544.

Orlova, A., and E. H. Egelman. 1992. Structural basis for the destabilization of F-actin by phosphate release following ATP hydrolysis. *J. Mol. Biol.* 227:1043–1053.

Orlova, A., and E. H. Egelman. 1993. A conformational change in the actin subunit can change the flexibility of the actin filament. *J. Mol. Biol.* 232:334–341.

Orlova, A., and E. H. Egelman. 1995. Structural dynamics of F-actin: I. Changes in the C-terminus. *J. Mol. Biol.* 245:582–597.

Orlova, A., E. Prochniewicz, and E. H. Egelman. 1995. Structural dynamics of F-actin: II. Cooperativity in structural transitions. *J. Mol. Biol.* 245:598–607.

Rayment, I., H. M. Holden, M. Whittaker, C. B. Yohn, M. Lorenz, K. C. Holmes, and R. A. Milligan. 1993. Structure of the actin-myosin complex and its implications for muscle contraction. *Science.* 261: 58–65.

Schutt, C. E., J. C. Myslik, M. D. Rozycki, N. C. W. Goonesekere, and U. Lindberg. 1993. The structure of crystalline profilin-β-actin. *Nature.* 365:810–816.

Schwyter, D., M. Phillips, and E. Reisler. 1989. Subtilisin-cleaved actin: polymerization and interaction with myosin subfragment 1. *Biochemistry.* 28:5889–5895.

Spudich, J. A., and S. Watt. 1971. The regulation of rabbit skeletal muscle contraction. I. Biochemical studies of the interaction of the tropomyosin-troponin complex with actin and the proteolytic fragments of myosin. *J. Biol. Chem.* 246:4866–4871.

Strzelecka-Golaszewska, H., J. Moraczewska, S. Y. Khaitlina, and M. Mossakowska. 1993. Localization of the tightly bound divalent-cation-dependent and nucletide-dependent conformation changes in G-actin using limited proteolytic digestion. *Eur. J. Biochem.* 211: 731–742.

Takashi, R. 1988. A novel actin label: a fluorescent probe at glutamine-41 and its consequences. *Biochemistry.* 27:938–943.

Tirion, M. M., D. ben-Avraham, M. Lopez, and K. C. Holmes. 1995. Normal modes as refinement parameters for the F-actin model. *Biophys. J.* 68:5–12.

Wu, P., and L. Brand. 1994. Resonance energy transfer methods and applications. *Anal. Biochem.* 218:1–13.

Zimmerle, C. T., K. Patane, and C. Frieden. 1987. Divalent cation binding to the high- and low-affinity sites on G-actin. *Biochemistry.* 26: 6545–6552.